Journal of the Korean Physical Society, Vol. 63, No. 3, August 2013, pp. 812∼816

Switchable Voltage Control of the Magnetic Anisotropy in Heterostructured Nanocomposites of CoFe/NiFe/PZT

Nguyen Thi Minh HONG, Nguyen Ba DOAN, Nguyen Huy TIEP,
Le Viet CUONG,* Bui Nguyen Quoc TRINH and Pham Duc THANG

Faculty of Engineering Physics and Nanotechnology and Laboratory for Micro and Nanotechnology, University of Engineering and Technology, Vietnam National University, Building E3, 144 Xuan Thuy Road, Cau Giay, Hanoi, Vietnam

Dong-Hyun KIM

Department of Physics, Chungbuk National University, Cheongju 361-763, Korea

(Received 31 May 2012)

In this work, we study the magnetic properties of a CoFe/NiFe/PZT heterostructured nanocomposite that is affected by the strain in the PZT substrate when a voltage in the range from –250 to 250 V is applied. An interesting electric-voltage-controlled magnetic anisotropy, with a relative increase in magnetization up to above 100%, is observed. This brings a new challenge to operate a low-power-consuming spin electronic device. We also utilize a theoretical model based on interface-charge-mediated and strain-mediated magnetic-electric coupling to understand the change in the magnetic properties of the investigated material.

PACS numbers: 77.84.-s, 77.65.-j, 75.50.Bb, 75.80.+q, 77.84.Lf, 75.85.+t
Keywords: Ferroelectrics, Ferromagnetics, Multiferroics, Nanocomposites
DOI: 10.3938/jkps.63.812

I. INTRODUCTION

Nanostructured composites of ferromagnetic (FM) and ferroelectric (FE) materials (multiferroics) are of increasing interest due to the coupling between the magnetic moments and the electric polarizations. In particular, the electric voltage, rather than the conventional magnetic field, can be directly used to control the magnetic property of multiferroic materials. The magnetic-electric (ME) coupling may open promising applications in novel spin electronic devices with low-power consumption. The electric-voltage-controlled magnetic anisotropy (EVCMA) can be achieved from the converse magnetoelectric effect (CME) in multiferroics [1–4]. Recently, several groups have demonstrated that a strain-induced ME coupling and an interface-charge-driven ME coupling coexist and interact with each other at the interface of the FM/FE heterostructures, which is evidence for an EVCMA behavior at room temperature [5–7].

In this work, we report a new finding of the CME and the EVCMA in the CoFe/NiFe/PZT heterostructured nanocomposite, whose FM material is CoFe/NiFe and whose FE material is PZT. Interestingly, we observe a switching of the magnetization at a suitable electric voltage. Furthermore, we study a theoretical model to understand the strain-induced magnetic anisotropy that originates from the coupling in the FM/FE heterostructures.

II. EXPERIMENTAL PROCEDURES

CoFe/NiFe/PZT heterostructured nanocomposites are fabricated as illustrated in Fig. 1; the 500- m-thick PZT

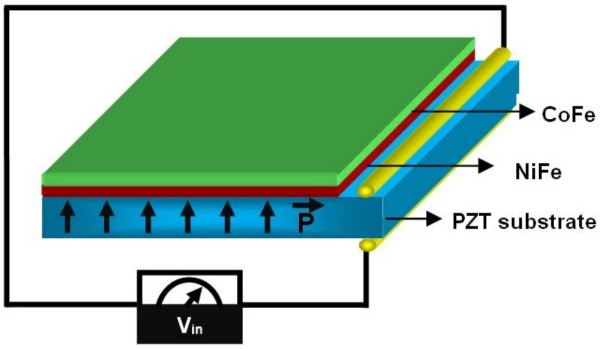

Fig. 1. (Color online) Geometry of the CoFe/NiFe/PZT heterostructure for the CME measurement.

*E-mail: pdthang@vnu.edu.vn

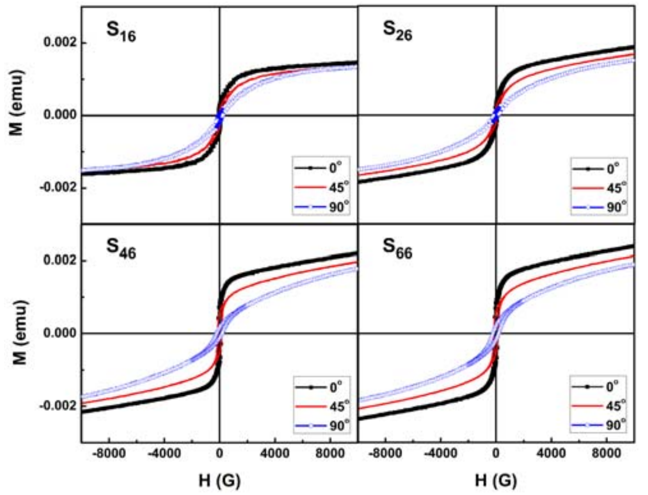

Fig. 2. (Color online) Magnetic hysteresis loops of samples measured at various angles α.

Table 1. Some characteristic magnetic properties of the samples.

Sample	$\mu_o H_c(G)$			$M_S(\mu$emu)		
	//	45°	90°	//	45°	90°
S_{16}	75	97	122	1458	1360	1340
S_{26}	100	120	163	1859	1662	1500
S_{46}	108	145	190	2175	1944	1758
S_{66}	116	152	197	2366	2093	1867

substrate has a polarization along the thickness direction. NiFe and CoFe ferromagnetic thin films were, in sequence, deposited at room temperature on the PZT by means of a magnetron sputter 2000-F system at an Ar pressure of 2.2 × 10^{-3} Torr and an rf- sputtering power of 50 W. In this study, the sputtering time was fixed to be 30 minutes for the CoFe layer, but was varied from 10, 20, 40 to 60 minutes for the NiFe layer, which are noted as samples S_{16}, S_{26}, S_{46} and S_{66}, respectively. The thickness of the FM thin films was changed up to 150 nm.

The CME and the EVCMA were characterized by using a vibrating sample magnetometer (VSM 7400). For these measurements, the sample was placed in an external magnetic field (H), and the applied voltage (V) were changed from –250 V to 250 V along the PZT thickness. The morphology and the crystallographic structure of the samples have been reported before [8]. The ferroelectric/piezoelectric properties of PZT were measured by using a ferroelectric tester (LC-10).

III. RESULTS AND DISCUSSION

Figure 2 shows the magnetic hysteresis curves $M(H)$ of the samples for various angles between the film-plane direction and the magnetic-field direction, α, where α = 0, 45 and 90°. The results imply that all samples have an in-plane magnetic anisotropy and a typical soft magnetic nature that originates from the contribution of the CoFe/NiFe layers. One observes that when the thickness of the NiFe layer is increased, both the saturation magnetization (M_S) and the coercivity ($H_{C\|}$) have an increasing tendency, as shown in Table 1. From this table, we can see that the sample S_{16} has the smallest M_S and $H_{C\|}$ among all the samples.

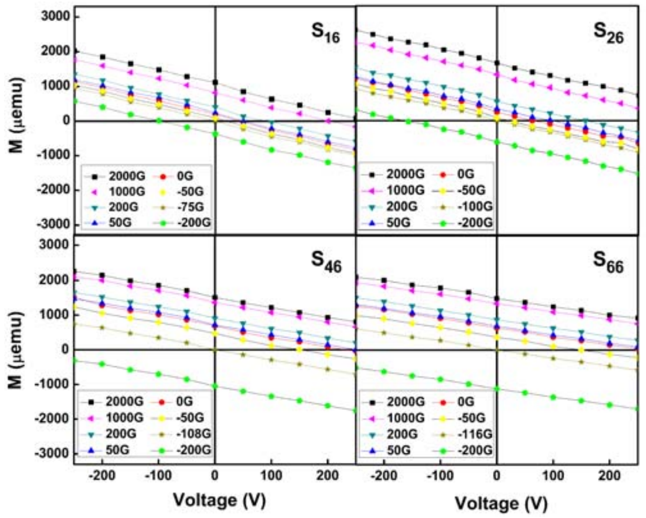

Fig. 3. (Color online) Dependences of the magnetization on the applied voltage $M(V)$ at different magnetic fields for all samples measured at α = 0°.

Table 2. Change in the magnetization ΔM, relative change in the magnetization M/ V, and magnetization reversed voltage V_{rev} of the samples (taken at –50 G).

Sample	ΔM (μemu)	$\Delta M/\Delta V$ (μemu/V)	V_{rev} (V)
S_{16}	804	4.02	16
S_{26}	650	3.25	35
S_{46}	610	3.05	165
S_{66}	540	2.70	190

Figure 3 shows the dependence of the magnetization on the voltage applied across the PZT substrate $M(V)$, which was measured at various H from –200 to 2000 G for α = 0°. In these cases, the voltage applied on the PZT substrate causes changes in the magnetization of the FM layers, and one can see that M decreases with increasing V, indicating that an elastic stress is transferred from the PZT substrate to the CoFe/NiFe thin film via the ME coupling. Note that the EVCMA of the FM/FE heterostructure depends not only on the material parameters and the FM/FE interface, but also on the direction of the applied voltage relative to the polarization direction in the FE layer. Thus, when a positive or negative voltage is applied, that is, parallel or anti-parallel to the polarization direction in the FE layer, an in-plane com-

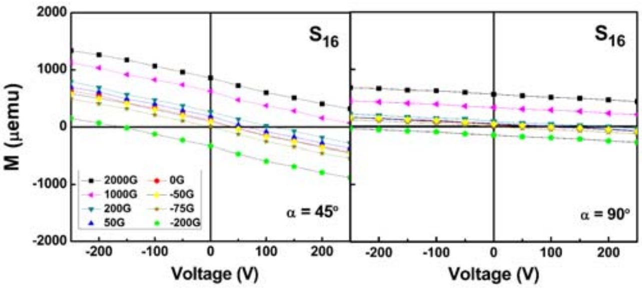

Fig. 4. (Color online) Angular dependence of the $M(V)$ curve measured at various magnetic field for sample S_{16}.

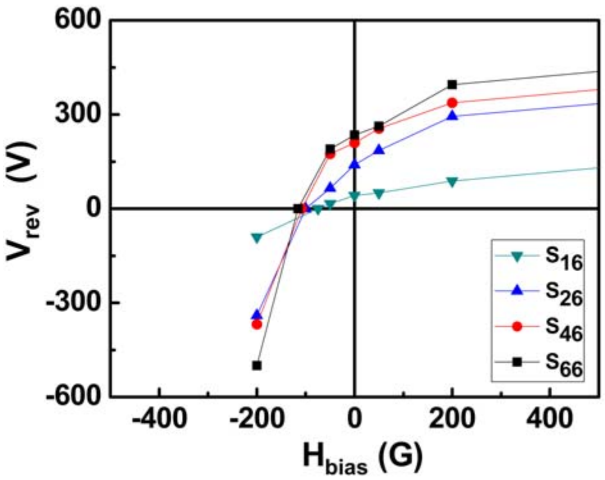

Fig. 5. (Color online) Relationship between the magnetization-reversed voltage and the bias magnetic field.

pressive or tensile stress, respectively, is generated. The stress is then transferred to the FM layers, leading to a change in the magnetization, ΔM [9]. The values of M and the relative change in the magnetization ($\Delta M/\Delta V$), measured at $\alpha = 0°$ and $H = –50$ G under a voltage in the range from –200 to 200 V, are enumerated in Table 2. We can see that ΔM and $\Delta M/\Delta V$ reach maximum values for sample S_{16} which has the thinnest thickness, which is due to the strain effect of the FM layers.

As shown in Fig. 4, the $M(V)$ curves still have a linearly decreasing tendency with increasing V for $\alpha = 45°$ and 90°. However, the value of ΔM decreases gradually as the magnetic-field direction deviates from the film-plane direction. Especially, the ΔM is very small at $\alpha = 90°$. For sample S_{16}, the values of ΔM are 804, 456 and 115 μemu for $\alpha = 0$, 45 and 90°, respectively, which is evidence for a relationship between the magnetization process and the direction of the applied magnetic field [10]. At $\alpha = 90°$, the relative change in magnetization is noted to be significant, up to above 100% at 250 V in an external magnetic field of 50 G.

Hereafter, we discuss the EVCMA. From Figs. 3-4, one can see that the magnetization can be reversed at a fixed voltage, which is denoted as V_{rev}. The values of

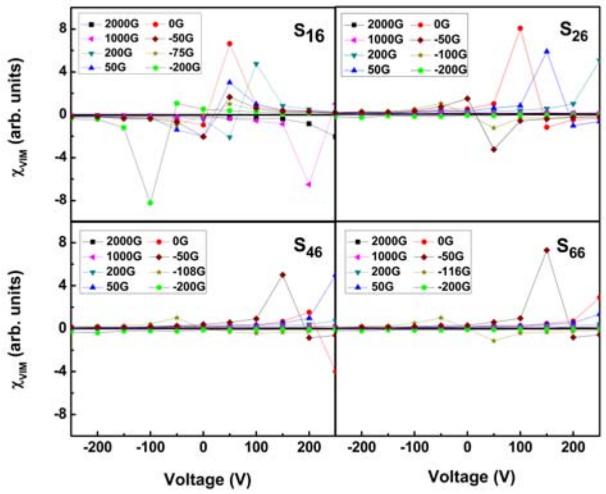

Fig. 6. (Color online) Magnetic field dependences of χ_{VIM} of samples measured at $\alpha = 0°$.

V_{rev} from Fig. 3 are plotted in Fig. 5 and listed in Table 2. Remarkably, V_{rev} changes with changing magnetic fields. Note that the thinner the thickness of the NiFe layer is, the smaller V_{rev} is. For sample S_{16}, the V_{rev} is smaller than it is for the others. As mentioned, sample S_{16} has the smallest magnetization; that is, the electric-voltage energy necessary to switch magnetic moment is the lowest. An interesting finding in Fig. 5 is the case with the bias magnetic field H_{bias} closes to $H_{C\|}$; one gets $V_{rev} = 0$, and while $H_{bias} \neq H_{C\|}$, V_{rev} is variable depending on the direction, as well as the magnitude, of the external magnetic field. Even without an external magnetic field, the application of a suitable voltage leading to a reverse magnetic order shows the possibility of magnetization switching.

To explain the above results in more detail, we calculate the voltage-induced magnetization susceptibility χ_{VIM} measured at various magnetic fields from –200 to 2000 G (see Fig. 6). Firstly, χ_{VIM} has a positive value at high applied voltage. With decreasing applied voltage, χ_{VIM} increases to a maximum, then goes to zero at V_{rev} and finally changes sign. The higher the bias magnetic field is, the higher required V_{rev} is, and this can be explained by using the magnetization process. At low fields, the magnetization process is mainly due to the orientations of the magnetic moments along the easy axis. With changing magnetic field, the magnetization increases due to the magnetization process. At higher fields, the magnetization rotates progressively from the easy axis to the field's direction. In this state, much higher energy is necessary to switch the magnetization. Therefore, the value V_{rev} increases with increasing H_{bias}. However, the magnetization only increases to a limit and reaches a saturation state. Once the magnetization is aligned along the direction of the magnetic field, the magnetization switching process no longer occurs, and χ_{VIM} approaches zero. Generally, magnetization switching can be decided by the competition between the magnetic-field energy and applied electric-voltage energy; *e.g.*, at $H = H_{C\|}$, $\chi_{VIM} = 0$ at $V = 0$. This evidence proves that only magnetic field energy and switch magnetization exist in this case. When $H_{bias} \neq H_{C\|}$, the value of χ_{VIM} varies and goes to zero at a suitable voltage that coincides with V_{rev}. Thus, at this moment, the applied electric-voltage energy is dominant and causes magnetization switching. The use of a suitable bias magnetic field plays an important role in the voltage-induced magnetization switching.

Recently, some reports have shown that two coupling mechanisms can coexist and tend to interact with each other at the interfaces of the FM/FE heterostructures; namely, interface-charge-mediated ME coupling and strain-mediated ME coupling [10–12]. The former mechanism is a direct voltage-induced modification of the magnetocrystalline anisotropy through a change in the interfacial spin configuration. For the later mechanism, an external voltage in the ferroelectric layer causes a strain change across the interface and then alters the magnetic anisotropy of the magnetic layer via magnetoelastic coupling. In the following, we demonstrate that in our heterostructures of CoFe/NiFe/PZT, the strain-mediated ME coupling mechanism dominates and contributes to the voltage-induced magnetic anisotropy.

By summing up the contributing magnetic anisotropies, such as the magnetocrystalline anisotropy, the magnetoelastic anisotropy and the surface anisotropy, the change in the total magnetic anisotropy energy of a ferromagnetic film can be derived as [13–16]

$$H_{eff}^{OP} = \frac{2K_1}{M_S} - \mu_0 M_S + \frac{2\left[B_1\left(1+\frac{2c_{12}}{c_{11}}\right)\varepsilon_0\right]}{M_S} + \frac{4K_S}{dM_S}\ , \quad (1)$$

where K_1, B_1 and K_S are the magnetocrystalline, magnetoelastic and surface anisotropic constants, c_{ij} (i, j = 1, 2) and ε_0 are the elastic stiffness constants and the residual strain in the ferromagnetic film, respectively, and d is the film's thickness.

An out of plane magnetic easy axis is preferred for $H_{eff}^{OP} > 0$, and a change in the sign of H_{eff}^{OP} from positive to negative indicates an easy axis reorientation from out of plane to in-plane or vice versa. The reorientation depends on the thickness of the magnetic thin films. The critical thickness d_{cr} when $H_{eff}^{OP} = 0$ is given by

$$D_{cr} = \frac{2K_S}{\frac{1}{2}\mu_0 M_S^2 - K_1 - B_1\left(1+\frac{2c_{12}}{c_{11}}\right)\varepsilon_0}\ . \quad (2)$$

On the other hand, the change in the total magnetic anisotropy under the application of a longitudinal electric voltage can be expressed as

$$\Delta H_{eff}^{OP} = \frac{H_{eff}^{OP}(V) - H_{eff}^{OP}(0)}{H_{eff}^{OP}(0)} = \frac{\frac{2\left[B_1\left(1+\frac{2c_{12}}{c_{11}}\right)\varepsilon_p(V) + \frac{\Delta K_S(V)}{d}\right]}{M_S}}{H_{eff}^{OP}}\ , \quad (3)$$

where ΔK_S is the change in the surface anisotropic constant under an external magnetic field.

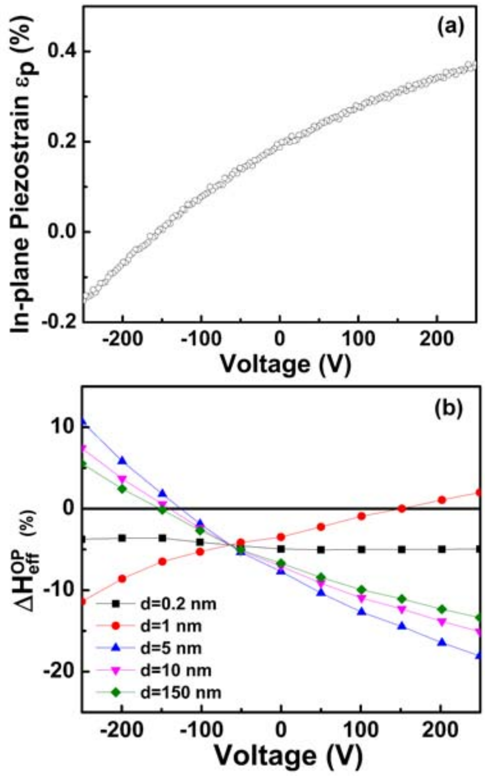

Fig. 7. (Color online) (a) The in-plane piezostrain ε_p generated in the PZT substrate. (b) Electric-voltage-induced change in the H_{eff}^{OP} of CoFe/NiFe/PZT heterostructures with various thicknesses of FM films.

The calculation for ΔH_{eff}^{OP} is performed by using Eq. (3) and the material parameters [17, 18]. The voltage dependences of the in-plane piezostrain ε_p of the PZT substrate and of the ΔH_{eff}^{OP} are illustrated in Fig. 7. For the CoFe/NiFe/PZT heterostructure, the critical thickness d_{cr} is 1.95 nm. The transition thickness d_{tr} for the two interacting ME coupling mechanisms at which the contributions from the two mechanisms become equal can be estimated to be about 0.2 nm. Hence, when the thickness of CoFe/NiFe is smaller than d_{tr}, the curve of ΔH_{eff}^{OP} tends to be a hysteresis-like loop, and the interface-charge ME coupling mechanism plays a major part. When the thickness of CoFe/NiFe exceeds the transition thickness d_{tr}, the curves of ΔH_{eff}^{OP} change to a butterfly shape, and the strain-mediated ME coupling takes place. Let us consider the variation of ΔH_{eff}^{OP} in a low electric-voltage range below 250 V, less than the ferroelectric coercive field of the PZT substrate (E_C = 5.2 kV/cm). As shown in Fig. 7(b), an asymmetric and monotonic decrease of $\Delta H_{eff}^{OP}(V)$ is observed for the CoFe/NiFe/PZT heterostructure. The opposite change trend for $\Delta H_{eff}^{OP}(V)$ from positive voltage to negative voltage is decided by the opposite signs of the induced in-plane piezostrains (Fig. 7(a)). Furthermore, taking the positive voltage part, the stress exerted by the PZT substrate is an in-plane compressive stress, and the CoFe/NiFe film has a positive magnetostriction constant, which would work against the easy magnetization axis being aligned along the in-plane direction. Hence, the observed decrease in ΔH_{eff}^{OP} is simliar to the change in the magnetization $M(V)$ and reflects the strain-mediated ME coupling, as well as electric-voltage-controlled magnetic anisotropy, in this heterostructure.

IV. CONCLUSION

The magnetic properties, including the CME and the EVCMA, of the CoFe/NiFe/PZT heterostructured nanocomposite have been studied. The effect of the electric voltage on the magnetic properties, with a relative increase in the magnetization of up to above 100%, is observed and explained based strain-mediated ME coupling. The results highlight a promising application to novel spin electronic devices with low power-consumption.

ACKNOWLEDGMENTS

This research was partly supported by project 103.02.87.09 of the National Foundation for Science and Technology Development (NAFOSTED) of Vietnam and by project QG.10.41 of the Vietnam National University in Hanoi.

REFERENCES

[1] Y. M. Jia, S. W. Or, H. L. W. Chan, X. Y. Zhao and H. S. Luo, Appl. Phys. Lett. **88**, 242902 (2006).
[2] Y. M. Jia, F. F. Wang, X. Y. Zhao, H. S. Luo, S. W. Or and H. L. W. Chan, Compos. Sci. Technol. **68**, 1440 (2008).
[3] S. Y. Chen, D. H. Wang, Z. D. Han, C. L. Zhang, Y. W. Du and Z. G. Huang, Appl. Phys. Lett. **95**, 022501 (2009).
[4] J. Lou, D. Reed, M. Liu and N. X. Sun, Appl. Phys. Lett. **94**, 112508 (2009).
[5] J. M. Hu, C. W. Nan and L. Q. Chen, Phys. Rev. B **83**, 134408 (2011).
[6] L. Shu, Z. Li, J. Ma, Y. Gao, L. Gu, Y. Shen, Y. Lin and C. W. Nan, Phys. Rev. **100**, 022405 (2012).
[7] T. H. E. Lahtinen, K. J. A. Franke and S. van Dijken, Sci.c Rep. **2**, 258 (2012).
[8] N. T. M. Hong, P. D. Thang, N. H. Tiep, L. V. Cuong and N. H. Duc, Adv. Nat. Sci.: Nanosci. Nanotechnol. **2**, 015015 (2011).
[9] N. T. M. Hong, N. H. Duc and P. D. Thang, Int. J. Nanotechnol. **10**, 206 (2013).
[10] M. Weisheit, Science **315**, 349 (2007).
[11] T. Maruyama, Y. Shiota, T. Nozaki, K. Ohta, N. Toda, M. Mizuguchi, A. A. Tulapurkar, T. Shinjo, M. Shiraishi, S. Mizukami, Y. Ando and Y. Suzuki, Nat. Nanotech. **4**, 158 (2009).
[12] M. Endo, S. Kanai, S. Ikeda, F. Matsukura and H. Ohno, Appl. Phys. Lett. **96**, 212503 (2010).
[13] J. M. Hu, Z. Li, J. Wang and C. W. Nan, J. Appl. Phys. **107**, 093912 (2010).
[14] J. M. Hu, Z. Li, J. Wang, J. Ma, Y. H. Lin and C. W. Nan, J. Appl. Phys. **108**, 043909 (2010).
[15] J. Wang, J. Ma, Z. Li, Y. Shen, Y. Lin and C. W. Nan, J. Appl. Phys. **110**, 043919 (2011).
[16] D. Peterka, A. Enders, G. Haas and K. Kern, Phys. Rev. B **66**, 104411 (2002).
[17] J. M. Hu and C. W. Nan, Phys. Rev. B **80**, 224416 (2009).
[18] D. Sander, A. Enders and J. Kirschner, J. Magn. Magn. Mater. **200**, 439 (1999).